Int. J. Electrochem. Sci., 11 **(2016)** 3039 - 3049

International Journal of
ELECTROCHEMICAL
SCIENCE
www.electrochemsci.org

Facile Synthesis of MoS_2 Modified TiO_2 Nanospheres with Enhanced Photoelectrocatalytic activity

Bin Dong[1,2,*], *Yan-Ru Liu*[1], *Guan-Qun Han*[1,2], *Wen-Hui Hu*[1], *Yong-Ming Chai*[1], *Yun-Qi Liu*[1,*], *Chen-Guang Liu*[1,*]

[1] State Key Laboratory of Heavy Oil Processing, China University of Petroleum (East China), Qingdao 266580, PR China
[2] College of Science, China University of Petroleum (East China), Qingdao 266580, PR China
[*]E-mail: dongbin@upc.edu.cn, liuyq@upc.edu.cn, cgliu@upc.edu.cn

Received: 3 September 2015 / *Accepted:* 3 February 2016 / *Published:* 1 March 2016

MoS_2/TiO_2 nanocomposites composed of MoS_2 nanosheets and TiO_2 nanospheres have been successfully prepared by a facile hydrothermal process. The as-prepared MoS_2/TiO_2 samples with different MoS_2 content have been characterized by scanning electron microscopy (SEM), X-ray diffraction (XRD) and transmission electron microscopy (TEM). The results show TiO_2 nanospheres with uniform size can improve the dispersion and decrease the aggregation of MoS_2 nanosheets. The best morphology and size of MoS_2/TiO_2 nanocomposites can be obtained when the content of MoS_2 is 70 wt% (M-7). UV-vis data show that MoS_2/TiO_2 samples have better absorption in visible light region compared to pure MoS_2 and TiO_2. The photoelectrocatalytic activity of MoS_2/TiO_2 samples has been evaluated by the photocurrent measurement. The results show that MoS_2/TiO_2 nanocomposites with MoS_2 content of 70 wt% (M-7) have the highest photocurrent which implies best photoelectrocatalytic activity of M-7. The reason may be that the suitable content of MoS_2 and the tight junction between MoS_2 and TiO_2 nanosphers is helpful for preventing the recombination of photogenerated electrons and holes.

Keywords: TiO_2 nanospheres; MoS_2; photoelectrocatalytic activity; nanocomposites

1. INTRODUCTION

Due to its earth-abundant reserves and low cost, MoS_2 with excellent electronic and optical properties has attracted much interests on hydrotreating catalysis [1], lithium ion battery [2], electrocatalytic hydrogen evolution reaction [3], photocatalytic degradation of organic pollutants [4-7] and optoelectronic devices [8-9]. Some research has found that with the stacking layers of MoS_2 decreasing to monolayer, an increasing could be observed from indirect band gap (1.29 eV) to direct

band gap (1.90 eV), which implies the betterd absorption in the visible light range [10-11]. Therefore, more and more researchers have focused their effort on the photocatalytic and photoelectrochemical property of MoS_2 as the alternatives of expensive Pt-based electrocatalysts [12-14].

Recently, the theoretical and experimental research has proved that active sites of layered MoS_2 are on the Mo-edges sites and the unsaturated sulfur atoms [15-16]. However, the 2D layered structure makes MoS_2 facile to aggregate and inefficiently adsorb reactant molecular because of its low specific surface area Furthermore, the more stacking layers of MoS_2 on 2D nanosheets, the less active sites. As a result, the catalytic activities dramatically decrease. Therefore, exposing more edges and rims of MoS_2 nanosheets can improve the catalytic activities. Many researches have been done to prepare novel nanostructure of MoS_2 [17-18] or hybrid nanomaterials [19-22] to increase the catalytic activity sites of MoS_2. Other than the number of active sites, the band gap of MoS_2 is also a key factor for photoelectrochemical HER. Owing to monolayer of MoS_2 has best absorption in visible light range, controlling the stacking of MoS_2 nanosheets is our goal.

In our work, MoS_2/TiO_2 nanocomposites have been synthesized via a simple hydrothermal reaction. TiO_2 nanospheres with uniform size and high area surface have been used as support to improve the dispersion and restrict the stacking numbers of MoS_2 nanosheets. The UV-vis and photocurrent measurements of the samples have been investigated in detail. The as-prepared MoS_2/TiO_2 nanocomposites exhibit higher photoelectrocatalytic activity for hydrogen evolution reaction.

2. EXPERIMENTAL SECTION

2.1 Preparation of TiO_2 nanospheres

The preparation of TiO_2 nanospheres references to a facile process reported by the literature [23]. The detailed method is as following: firstly, 5 ml tetrabutoxytitanium was added into 50 ml ethylene glycol ($(CH_2OH)_2$), and the mixture solution was stirred for 8 h. Then 200 ml acetone was poured into the former mixture solution under stirring for 1h. The obtained white precipitates were washed and dried at 60 ℃ overnight. Then titanium glycolate precursor was obtained. Next, 0.300 g titanium glycolate precursor was added into 60 ml deionized water, and refluxed for 1h at 80 ℃. The white precipitates were washed and dried at 60 ℃ overnight. Finally the white TiO_2 nanopheres were obtained.

2.2 Preparation of MoS_2/TiO_2 nanocomposites

MoS_2/TiO_2 nanocomposites (70 wt% of MoS_2, denoted as M-7) were preparated via a hydrothermal method. Firstly, 0.06 g sodium molybdate ($NaMoO_4{\cdot}2H_2O$) and 0.12 g thiourea (C_2H_5NS) were dispersed in 70 ml deionized water. Then 0.013 g TiO_2 nanospheres were added into the above solution and stirred for 0.5 h. The obtained suspension was transferred into a Teflon-lined stainless steel autoclave and then heated in an electric oven at 220 ℃ for 24 h. The black precipitates

were washed and dried at 50 ℃ overnight. Following the above mentioned procedure, MoS_2/TiO_2 nanocomposites with different content (50 wt%, 90% of of MoS_2, denoted as M-5 and M-9) were also prepared. For comparison, the pure MoS_2 was prepared under the identical conditions.

2.3 Photoelectrochemical tests

The photoelectrochemical characterization of the different samples have been measured by electrochemical workstation (CHI 604E, Chenhua, China) with a three-electrode composed of FTO electrode decorated by different MoS_2/TiO_2 nanocomposites as working electrode, platinum foil as the auxiliary electrode, and a silver chloride electrode (Ag/AgCl) as a reference electrode. The working electrodes were prepared as follows: 20 mg of the samples were dispersed in 2 ml absolute ethanol of Nafion to obtain samples slurry. Then, the slurry was dropped onto a 1.5 cm×1.0 cm F-doped SnO2-coated glass (FTO glass) electrode. Next, these electrodes were dried in an oven at 60 °C for 3 h. All the measurements were carried out in the aqueous solution of 0.35 M/0.25 M Na_2S-Na_2SO_3 without bias potential at room temperature. A 100 W xenon lamp with visible light wavelength range has been used as light source with 50 mW/cm^2 incident light intensity to measure the photoelectrochemical properties.

2.4 Characterization

Crystallographic structure of all as-prepared samples was investigated with X-ray powder diffraction (XRD, X'Pert PRO MPD, Cu KR) at a scanning rate of 1 °C min-1. XRD data were collected in the 2θ ranges from 5 to 76°. The morphology of the samples was examined with field-emission scanning electron microscopy (SEM, Hitachi, S-4800). Transmission electron microscopy (TEM) images were collected on HRTEM, JEM-2100UHR with an accelerating voltage of 200 kV. The samples were prepared by dropping the ethanol solution of samples on the Cu grids. UV-vis pectra were recorded on a UV-vis spectrometer (UV-
2600, Shimadzu, Japan) over a spectral range of 200-1000 nm.

3. RESULTS AND DISCUSSION

X-ray diffraction (XRD) patterns of pure MoS_2, M-7 and TiO_2 nanaospheres are shown in Figure 1. As for pure MoS_2 sample (curve a in Figure 1), the (002), (100), (103), (110) planes corresponding peaks can be assigned to 14.1°, 32.9°, 39.5° and 58.8°(JCPDS 01-075-1539), respectively.

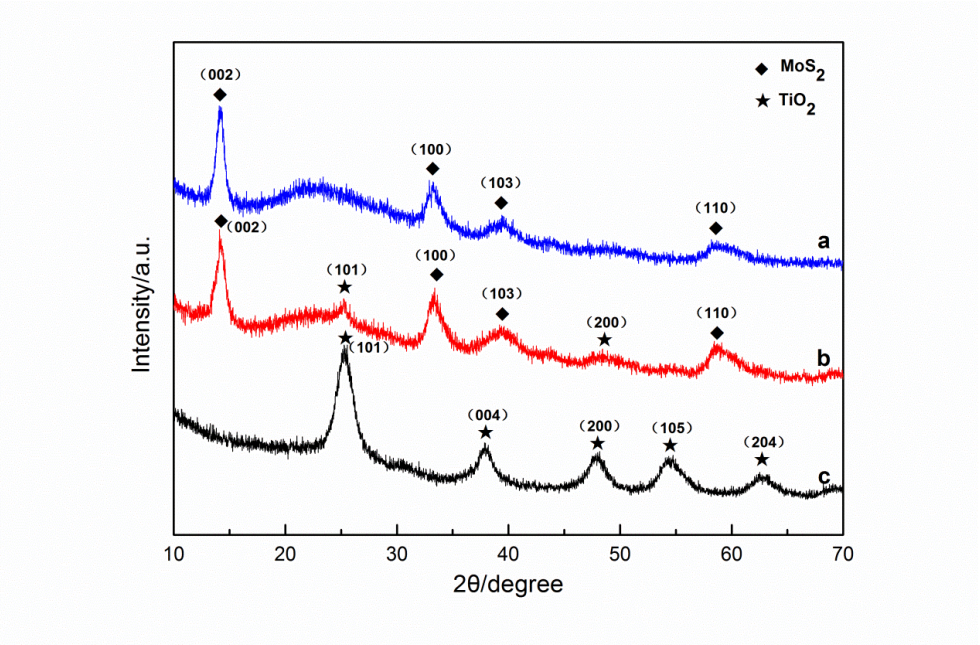

Figure 1. XRD data of the different samples: (a) pure MoS_2; (b) MoS_2/TiO_2 (M-7) and (c) pure TiO_2.

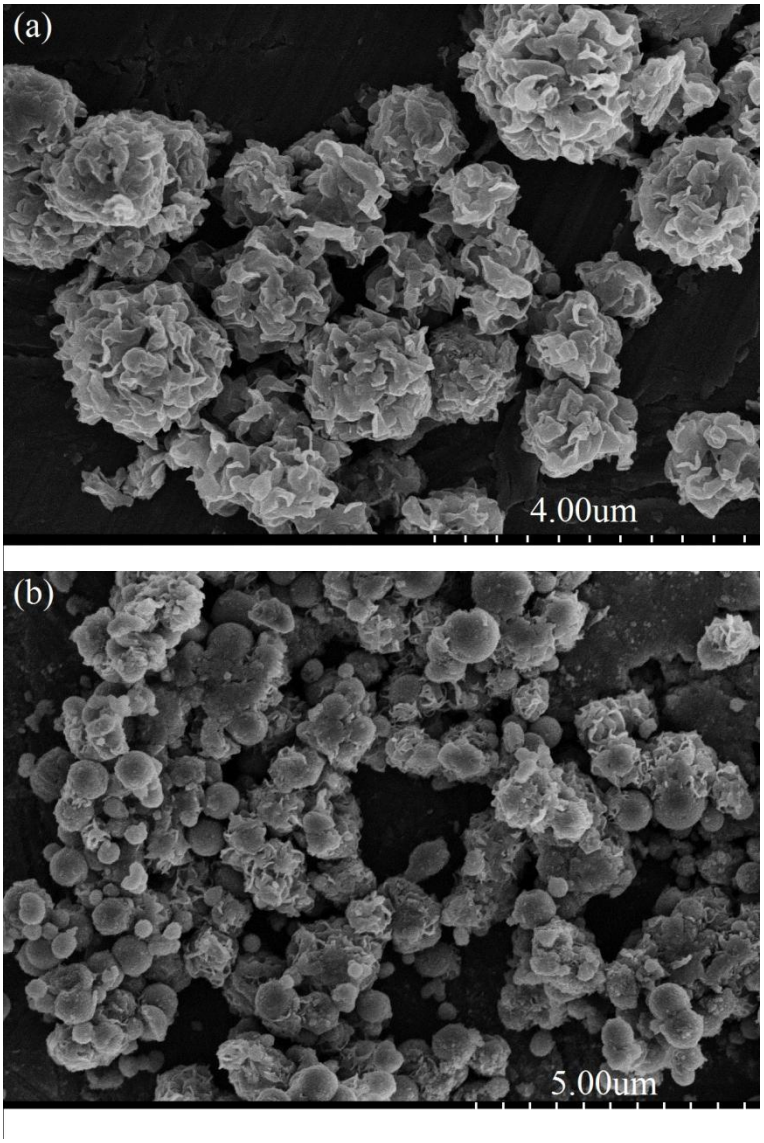

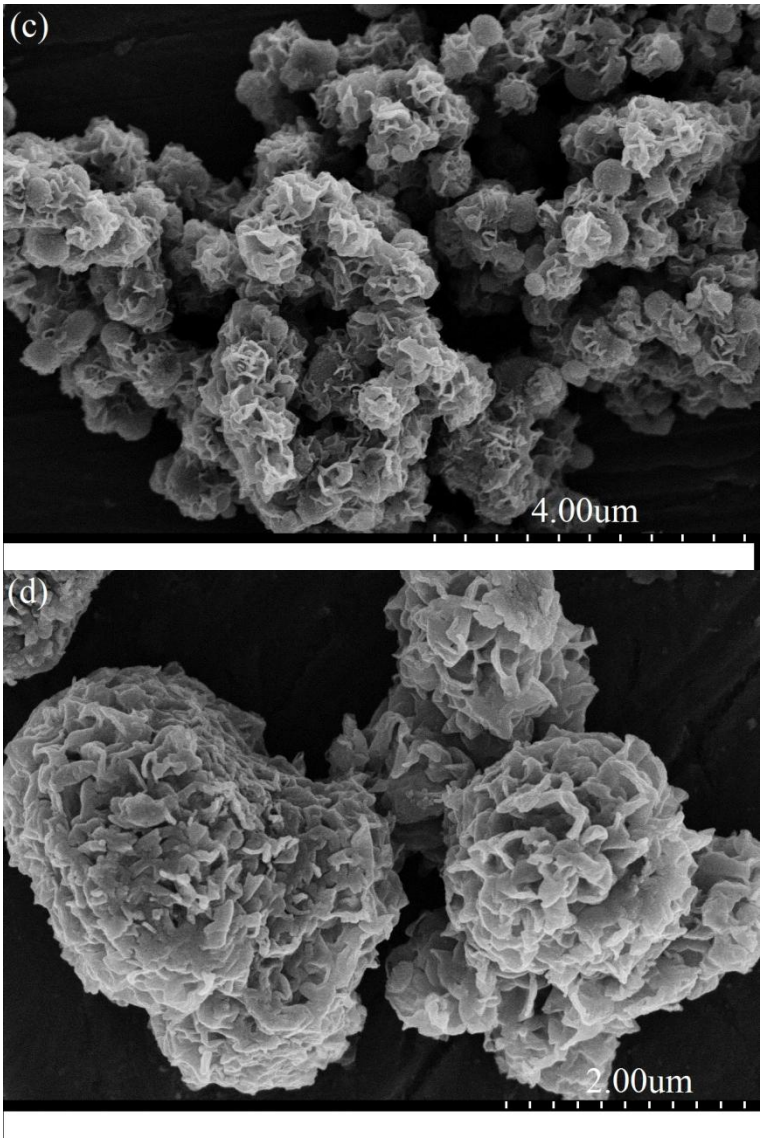

Figure 2. SEM images of the different samples: (a) pure MoS_2; (b) MoS_2/TiO_2(M-5); (c) MoS_2/TiO_2 (M-7); (d) MoS_2/TiO_2 (M-9).

It can be seen that the peak at 14.1°become weaker in M-7 (curve b in Figure 1) than that in pure MoS_2, indicating that TiO_2 nanospheres restrict the growth along (002) plane of MoS_2. The stacking layers of MoS_2 will decrease with the weakness of (002), which implies that the MoS_2 in M-7 can expose more edges and rims as catalytic sites. The diffraction peaks of the pure TiO_2 nanospheres (curve c in Figure 1) are in keeping with the peaks of the standard pure anatase TiO_2 (JCPDS: 01-071-1167). The broader peaks of (101), (004), (200), (204) indicate that TiO_2 nanospheres have the amorphous state and low crystalline.

Figure 2a displays the corresponding SEM image of pure MoS_2. The pure MoS_2 obtained by the same hydrothermal method have the nanoflower morphology of with the severe stacking and large size of the diameter of 2 um. SEM image of M-5 (with 50 wt% of MoS_2) is shown in Figure 2b. Absolutely, only few TiO_2 nanospheres can be decorated by MoS_2. The MoS_2/TiO_2 nanocomposites

can't be successfully synthesized when adding 50 wt% of MoS_2. Compared to M-5, TiO_2 nanospheres in M-7 with the diameter of 0.5 um were mostly packaged by MoS_2, and the nanocomposites of M-7 exhibit the spherical shape with good distribution and similar size (in Figure 2c).

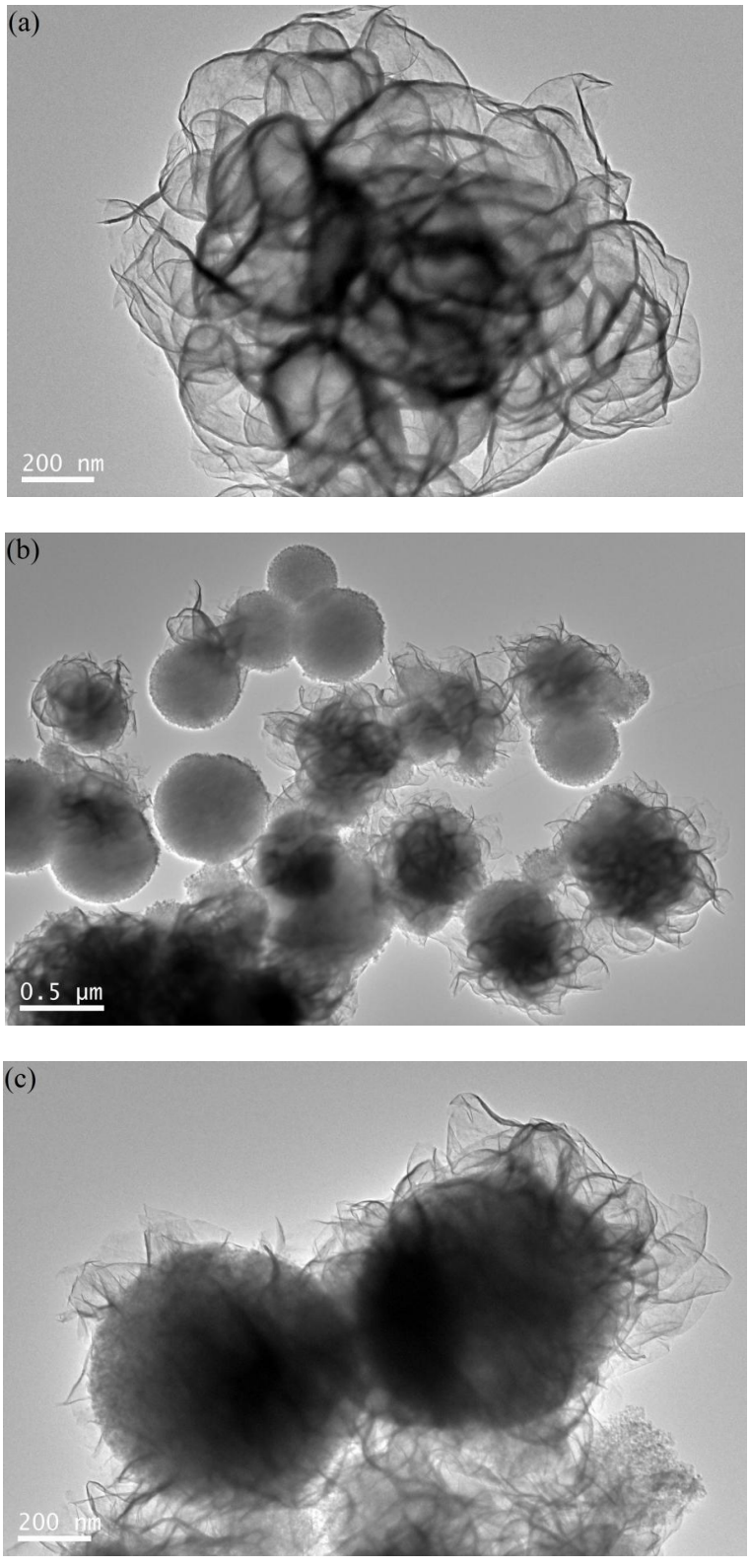

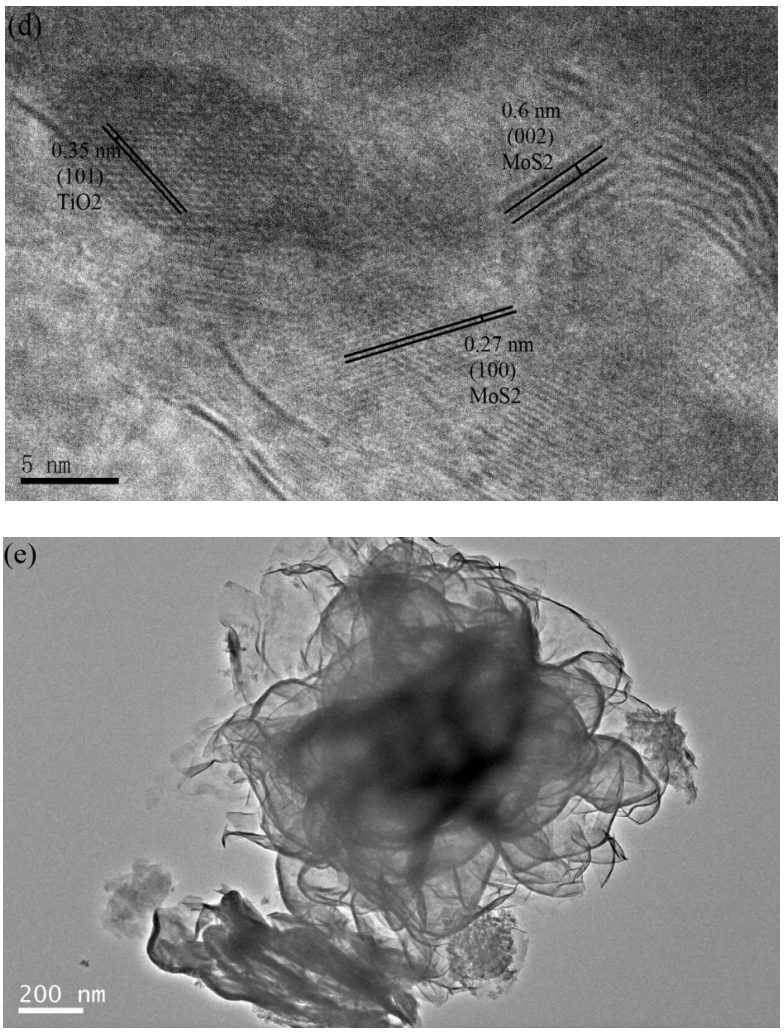

Figure 3. TEM images of the different samples: (a) pure MoS_2; (b) MoS_2/TiO_2(M-5); (c) MoS_2/TiO_2 (M-7); (d) HRTEM of M-7; (e) MoS_2/TiO_2 (M-9).

It can be seen that MoS_2 homogenously disperse on the surface of TiO_2 nanospheres which means that the MoS_2/TiO_2 composites are prepared successfully. When increasing the content of MoS_2 to 90% in M-9, the obvious stacking of MoS_2 sheets can be observed in Figure 2d. The diameter of M-9 also increases to about 2 μm, which may be caused by the excess of MoS_2. Therefore, M-7 have the better morphology and junction between MoS_2 and TiO_2.

Transmission electron Microscopy (TEM) images of the different samples are displayed in Figure 3. Figure 3a shows the typical stacking morphology of pure MoS_2 nanosheets. Obviously, pure MoS_2 grow rapidly and have severe aggregation in the absence of TiO_2 nanospheres. When adding TiO_2 nanospheres to synthesize M-5, only few MoS_2/TiO_2 nanocomposites can be seen in Figure 3b, which is identified by SEM image in Figure 2b. Figure 3c shows the TEM image of M-7, indicating that the few layers of MoS_2 nanosheets can homogenously grow on the surface of TiO_2 nanospheres with the small diameter of 0.5 μm. A high-resolution TEM (HRTEM) image (Figure 3d) also revealed the tight recombination between MoS_2 and TiO_2. Under higher resolution, the layered structure of MoS_2 nanosheets with an average spacing of 0.6 nm can be seen, which belongs to the (002) facet of MoS_2. The crystallographic spacing of 0.27 nm corresponds to the lattice parameter in the (100) plane

of MoS_2. Furthermore, the lattice spacing of 0.35 nm is equal to the (101) plane of TiO_2. These results proved that the good junction of MoS_2 and TiO_2 can be obtained when the content of MoS_2 is 70 wt%. When the content of MoS_2 is up to 90%, the severe stacking of MoS_2 nanosheets and the larger size can be observed in Figure 3e.

The structure and properties of photoelectrocatalysts related to bandgap, size, and/or band positionhas important effect on the absorption properties. UV-vis absorption measurement has been used to evaluate bandgaps of the different samples.

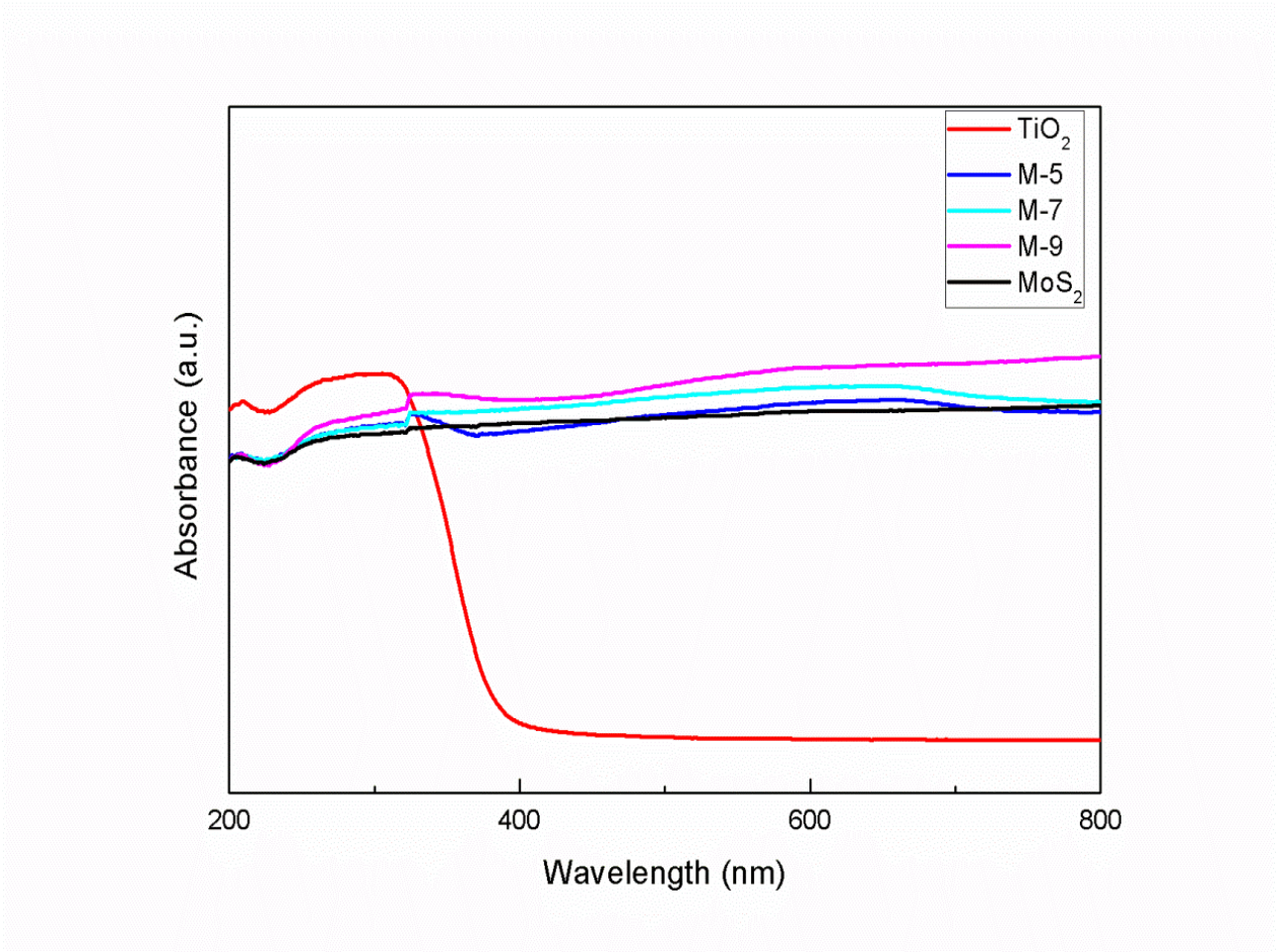

Figure 4. UV-vis absorption spectra of TiO_2 nanospheres; MoS_2/TiO_2(M-5); MoS_2/TiO_2 (M-7); MoS_2/TiO_2 (M-9) and pure MoS_2.

As shown in Figure 4, the pure TiO_2 nanospheres only have the basic absorption band in UV light range. Either pure MoS_2 or MoS_2/TiO_2 nanocomposites show enhanced absorption in visible light region. Compared with the TiO_2 nanoapheres' calculated bandgap energy (3.20 ev) , the bandgap energy of MoS_2/TiO_2 nanocomposites is close to 2.80 ev. This proves the as-prepared MoS_2/TiO_2 nanocomposites is very suitable for photoelectrocatalytic HER [24].

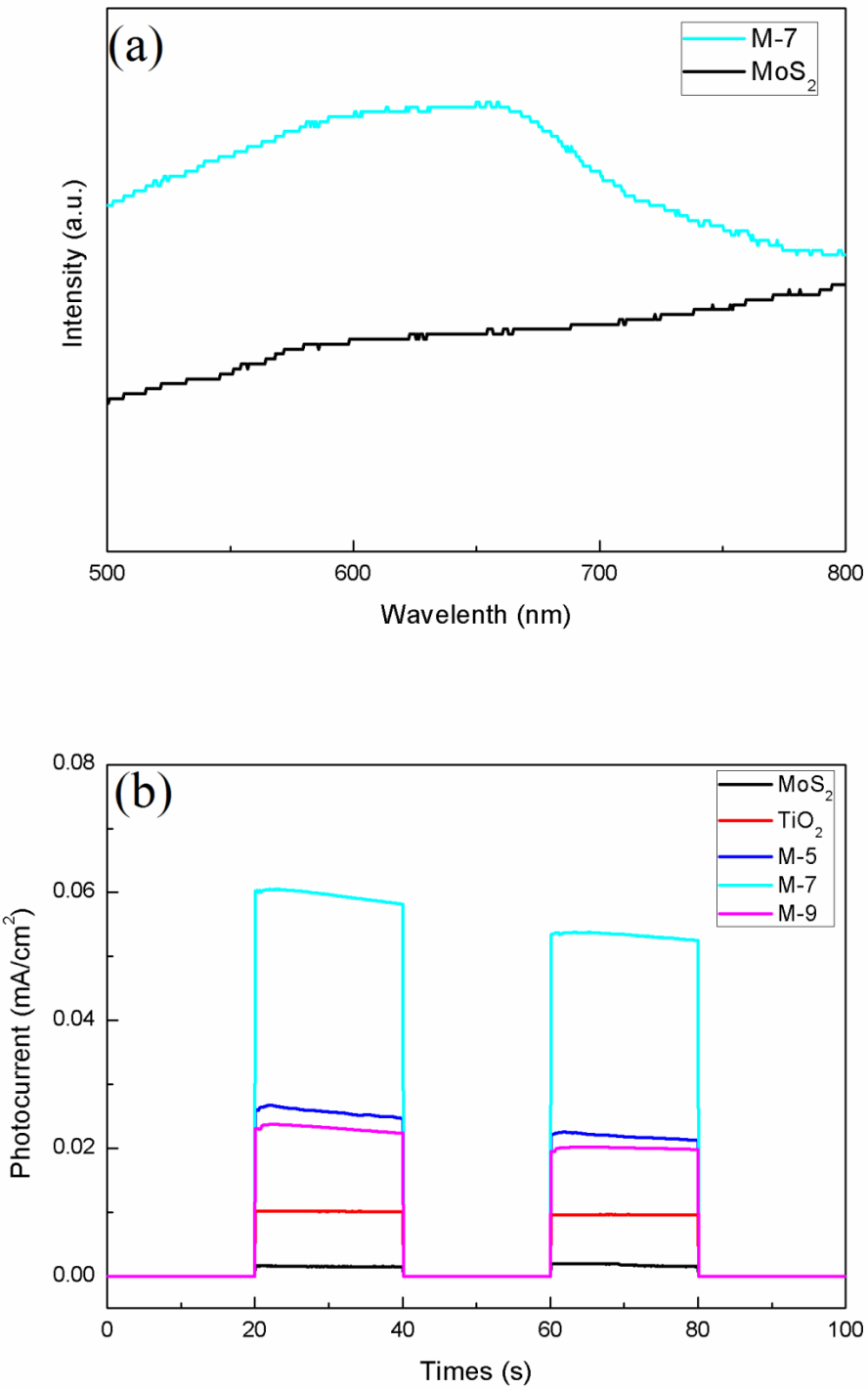

Figure 5. (a) Photoluminescence spectra of pure MoS_2 and MoS_2/TiO_2 (M-7); (b) The photocurrent measurements of TiO_2 nanospheres; MoS_2/TiO_2(M-5); MoS_2/TiO_2 (M-7); MoS_2/TiO_2 (M-9) and pure MoS_2.

It has been proved that MoS_2 monolayer has the strongest photoluminescence (PL) absorption compared to the bulk MoS_2 [25]. A board peak centered at 650 nm (1.92 eV) can be observed on MoS_2/TiO_2 nanocomposites in Figure 5a. The band gap energies of about 1.9 eV proved the existence

of MoS_2 monolayer structure [26]. In addition, the absorption intensity of MoS_2/TiO_2 nanocomposites is higher than that of pure MoS_2, indicating well dispersion of MoS_2 in the nanocomposites than in the pure MoS_2.

In order to characterize the different samples' ability of separating of photogenerated electrons and producing charge carriers, the photocurrent measurements are used. As shown in Figure 5b, M-7 shows the strongest photocurrent intensity than pure MoS_2, TiO_2 and M-5, M-9. Therefore, the results imply that M-7 has better structure and tends to easier produce charge carriers and separated electrons. Because the presence of photogenerated electrons is the key factor in actual photocatalytic HER performance, MoS_2 in M-7 can transfer more photogenerated electrons to protons for improving hydrogen evolution reaction. So M-7 is expected to exhibit enhanced photocatalytic activity for HER.

4. CONLUSIONS

Novel MoS_2/TiO_2 nanocomposites with well dispersed MoS_2 nanosheets on the surface of TiO_2 nanospheres have been successfully synthesized via a facile hydrothermal reaction. The morphology and structure of MoS_2/TiO_2 nanocomposites have been characterized. The loading of MoS_2 can impact the dispersion and junction of the nanocomposites. The M-7 with the 70 wt% content of MoS_2 has the best dispersion and heterostructure, which is helpful to improve the photocatalytic H_2 production activity. UV-vis and the photocurrent tests also proved the best photoelectrochemical activity of M-7. The unique heterostructure composed of MoS_2 and TiO_2 nanospheres break new grand in designing newfangled hierarchical MoS_2-based photoelectrocatalysts for HER.

ACKNOWLEDGEMENTS
This work is financially supported by the National Natural Science Foundation of China (U1162203 and 21106185) and the Fundamental Research Funds for the Central Universities (15CX05031A).

References

1. R.R. Chianelli, G. Berhault and B. Torres, *Catal. Today*, 147 (2009) 275.
2. J. Cho, H. Hwang and H. Kim, *Nano Lett.*, 11 (2011) 4826.
3. C.G. Morales-Guio, L. A. Stern and X.L. Hu, *Chem. Soc. Rev.*,43 (2014) 6555.
4. Q. Xiang, J. Yu and M. Jaroniec, *J. Am. Chem. Soc.*, 134(15) (2012) 6575.
5. F.A. Frame and F. E. Osterloh, *J. Phys. Chem. C*, 114(23) (2010) 10628.
6. W.J. Zhou, Z.Y. Yin, Y.P. Du, X. Huang, Z.Y. Zeng, Z.X. Fan, H. Liu, J.Y. Wang and H. Zhang, *Small*, 9 (2013) 140.
7. H. Zhao, Y. Dong, P. Jiang, H. Miao, G. Wang and J. Zhang, *J. Mater. Chem. A*, 3(14) (2015) 7375.
8. H. S. Lee, S. W. Min, Y. G. Chang, M. K. Park, T. Nam, H. Kim, J. H. Kim, S. Ryu and S. Im, *Nano Lett.*, 12 (2012) 3695.
9. O. Lopez-Sanchez, D. Lembkel, M. Kayci, A. Radenovic and A. Kis, *Nat. Nanotechnol.*, 8 (2013) 497.
10. T.S. Li and G.L. Galli, *J. Phys. Chem. C*, 111 (2007) 16192.
11. C. Lee, H. Yan, L.E. Brus, T. F. Heinz, J. Hone and S. Ryu, *ACS Nano*, 4 (2010) 2695.

12. G. J. Zhou, Y. M. Xu, Y. Z. Fu, Y. Yang and Y. C. Zhang, *Int. J. Electrochem. Sci.*, 9 (2014) 3990.
13. Y. Z. Song, W. H. Song, L. Qian, J. H. Wang, X. M. Zhang, X. M. Lv and J. M. Xie, *Int. J. Electrochem. Sci.*, 9 (2014) 6843.
14. Y. G. Li, H. L. Wang, L. M. Xie, Y. Y. Liang, G. S. Hong and H. J. Dai, *J. Am. Chem. Soc.*, 133 (2011) 7296.
15. B. Hinnemann, P. G. Moses, J. Bonde, K. P. Jørgensen, J. H. Nielsen, S. Horch, I. Chorkendorff and J. K. Nørskov, *J. Am. Chem. Soc.*, 127 (2005) 5308.
16. T. F. Jaramillo, K. P. Jorgensen, J. Bonde, J. H. Nielsen, S. Horch and I. Chorkendorff, *Science*, 317 (2007) 100.
17. M. Remskar, A. Mrzel, Z. Skraba, A. Jesih, M. Ceh, J. Demsar, P. Stadelmann, F.Levy and D. Mihailovic, *Science*, 292 (2001) 479.
18. G. Nagaraju, C. Tharamani, G. Chandrappa and J. Livage, *Nanoscale Res. Lett.*, 2 (2007) 461.
19. Q. Xiang, J. Yu and M. Jaroniec, *J. Am. Chem. Soc.*, 134 (2012) 6575.
20. S. Min and G. Lu, *J. Phys. Chem. C*, 116 (2012) 25415.
21. C. Liu, L. Wang, Y. Tang, S. Luo, Y. Liu, S. Zhang, Y. Zeng and Y. Xu, *Appl. Catal. B*, 164 (2015) 1.
22. Meng Shen, Zhiping Yan, Lei Yang, Pingwu Du, Jingyu Zhang and Bin Xiang, *Chem. Commun.*, 50 (2014) 15447.
23. J. Brivio, D.T. Alexander and A. Kis, *Nano Lett.*, 11 (2011) 5148.
24. M. Weber and M. Dignam, *Int. J. Hydrogen Energy*, 11 (1986) 225.
25. J.Z. Ou, A.F. Chrimes, Y. Wang, S.Y. Tang, M.S. Strano and K. Kalantar-Zadeh, *Nano Lett.*, 14 (2014) 857.
26. E.S. Kadantsev and P. Hawrylak, *Solid State Commun.*, 152 (2012) 909.

© 2016 The Authors. Published by ESG (www.electrochemsci.org). This article is an open access article distributed under the terms and conditions of the Creative Commons Attribution license (http://creativecommons.org/licenses/by/4.0/).